

Flexoelectric effects in liquid crystals formed by pear-shaped molecules. A computer simulation study

Joachim Stelzer^{*}, Roberto Berardi, Claudio Zannoni

Dipartimento di Chimica Fisica ed Inorganica, Università, Viale Risorgimento, 4, 40136 Bologna, Italy

Received 17 August 1998; in final form 12 October 1998

Abstract

The flexoelectric effect in liquid crystals is investigated by means of Monte Carlo simulations for model pear-shaped molecules that interact through a combination of Gay–Berne and Lennard-Jones potentials. Flexoelectric coefficients are evaluated from microscopic expressions derived on the basis of a density functional approach. © 1999 Elsevier Science B.V. All rights reserved.

1. Introduction

The flexoelectric effect in liquid crystals [1] concerns the linear coupling of *splay* and *bend* director deformations to an electric polarization. Flexoelectric liquid crystal materials exhibit a polarization \mathbf{P} proportional to the orientational deformation of the director field \mathbf{n} ,

$$\mathbf{P} = e_{11} \mathbf{n} \operatorname{div} \mathbf{n} + e_{33} \mathbf{n} \times \operatorname{curl} \mathbf{n}, \quad (1)$$

where e_{11} and e_{33} denote the flexoelectric coefficients related to *splay* and *bend* distortions, respectively. The phenomenon is somewhat similar to the piezoelectric effect in certain solid crystals where a coupling between mechanical stress and polarization is observed, so that the polarization manifests itself due to a positional deformation. The flexoelectric effect has attracted a great deal of attention because of its possible applications in transducers and, generally, in electro-optical devices. However, and more

importantly here, there is also a fundamental interest, as the relation between the flexoelectric coefficients and molecular structure is far from being understood. Meyer in his seminal paper [1] showed that a geometrical asymmetry of the mesogen molecules, or ‘shape polarity’, should lead to a non vanishing effect. He used as explicit examples wedge-shaped (‘pear’) and bow-shaped (‘banana’) molecules. These are of course not the only molecular shapes allowing the effect and Prost and Marcerou [2,3] and Osipov [4,5], in particular, have considered quadrupolar-like flexoelectricity. From the theoretical point of view microscopic theories of the effect have been developed at the molecular field level by Straley [6] and Osipov [5]. A linear response formalism relating a third rank flexoelectric tensor to correlations of torque flux and polarization has been given by Nemtsov and Osipov [7]. Rather surprisingly, investigations in terms of computer simulations are not yet available. Here we address the problem of relating molecular shape and flexoelectricity by Monte Carlo simulations, introducing a simple model of pear-shaped

^{*} Corresponding author. E-mail: joachim@ms.fci.unibo.it

molecules built from a Gay–Berne and a Lennard–Jones center. This will allow us to change easily and in a controlled way the molecular shape asymmetry. We also develop non mean-field microscopic expressions for the flexoelectric coefficients in terms of suitable averages over the direct pair correlation function, thus generalizing the approach by Straley [6]. Finally, we estimate these coefficients from simulation results.

2. Microscopic expressions for flexoelectric coefficients

We start writing the distortion induced polarization \mathbf{P} as an average of the molecular steric dipoles $\mathbf{p}_i = p \mathbf{u}_i$, of strength p , over the orientational distribution function (ODF), $f(\mathbf{u}_i)$, of the molecular axes \mathbf{u}_i ,

$$\begin{aligned} \mathbf{P} &= \rho p \int d\mathbf{u}_i f(\mathbf{u}_i) \mathbf{u}_i \\ &= \rho p \int d\mathbf{u}_i f_0(\mathbf{u}_i) \delta f(\mathbf{u}_i) \mathbf{u}_i, \end{aligned} \quad (2)$$

where ρ is the number density and we have assumed that $f(\mathbf{u}_i)$ can be expressed by its uniaxial equilibrium feature, $f_0(\mathbf{u}_i)$, which is altered by a slight perturbation $\delta f(\mathbf{u}_i)$, i.e., $f = f_0(1 + \delta f)$ [6]. According to Straley [6], this perturbation can be determined by variational calculus from the functional derivative of the total free energy, giving

$$\begin{aligned} \delta f(\mathbf{u}_i) &= \rho \int d\hat{\mathbf{r}}_{ij} d\mathbf{u}_j c(\mathbf{r}_{ij}, \mathbf{u}_i, \mathbf{u}_j) (\mathbf{r}_{ij} \cdot \nabla) \\ &\quad \times f_0(\mathbf{u}_j). \end{aligned} \quad (3)$$

In Eq. (3) $c(\mathbf{r}_{ij}, \mathbf{u}_i, \mathbf{u}_j)$ is the direct pair correlation function (DPCF) which depends on \mathbf{u}_i , \mathbf{u}_j and on the separation vector \mathbf{r}_{ij} of a pair of molecules. The gradient of f_0 in Eq. (3) can be expressed by director gradients when assuming that the distribution is locally at equilibrium [8]. This means that the orientations of the molecular axes follow the local director, and hence $f_0(\mathbf{u}_j) = f_0(\mathbf{n}(\mathbf{r}) \cdot \mathbf{u}_j)$. Following e.g., Ref. [8–10], the DPCF does not contain a director dependence. This is compatible with a sys-

tem where the local uniaxial director is isotropically distributed for a sufficiently large sample or, equivalently, fluctuates in time to maintain the overall isotropic symmetry, appropriate in the absence of a symmetry breaking field. For further considerations we choose the local coordinate system (at point \mathbf{r}) so that $\mathbf{n}(\mathbf{r}) = \hat{\mathbf{z}}$ and \mathbf{u}_j lies in the xz plane [6]. By this simplification the gradient of the ODF can be expressed as

$$\begin{aligned} \nabla f_0(\mathbf{n}(\mathbf{r}) \cdot \mathbf{u}_j) &= f'_0(\cos \beta_j) u_{j,x} \\ &\quad \times (\mathcal{S} \hat{\mathbf{x}} + \mathcal{T} \hat{\mathbf{y}} + \mathcal{B} \hat{\mathbf{z}}), \end{aligned} \quad (4)$$

where \mathcal{S} , \mathcal{T} , \mathcal{B} are the amplitudes of *splay*, *twist* and *bend* distortions, respectively, and $f'_0(\cos \beta_j)$ denotes the derivative of the uniaxial ODF with respect to its argument (β_j is the angle between molecule j and the director). Inserting Eqs. (3) and (4) in Eq. (2) we obtain the microscopic analogue of Eq. (1) and by comparison we can find the expressions for the flexoelectric coefficients:

$$\begin{aligned} e_{11} &= \rho^2 p \int d\mathbf{r}_{ij} d\mathbf{u}_i d\mathbf{u}_j f_0(\cos \beta_i) u_{i,z} \\ &\quad \times f'_0(\cos \beta_j) u_{j,x} r_{ij,x} c(\mathbf{r}_{ij}, \mathbf{u}_i, \mathbf{u}_j), \end{aligned} \quad (5)$$

$$\begin{aligned} e_{33} &= \rho^2 p \int d\mathbf{r}_{ij} d\mathbf{u}_i d\mathbf{u}_j f_0(\cos \beta_i) u_{i,x} \\ &\quad \times f'_0(\cos \beta_j) u_{j,x} r_{ij,z} c(\mathbf{r}_{ij}, \mathbf{u}_i, \mathbf{u}_j). \end{aligned} \quad (6)$$

The structure of these expressions is similar to the Poniewierski–Stecki expressions [8,9] which establish a microscopic route to the Frank elastic constants [11]. In our approach the flexoelectric coefficients arise from averages over molecular pair correlations. In order to use the expressions (5) and (6) for practical calculations we have to perform the required averages. To do this we expand $f_0(\mathbf{u}_j)$ and $c(\mathbf{r}_{ij}, \mathbf{u}_i, \mathbf{u}_j)$ in spherical harmonics, $Y_{L,m}$. The expansion of the DPCF reads [12]

$$\begin{aligned} c(\mathbf{r}_{ij}, \mathbf{u}_i, \mathbf{u}_j) &= \sum_{\substack{L_1, L_2, L \\ m_1, m_2}} c_{L_1, L_2, L}(r_{ij}) \\ &\quad \times C(L_1, L_2, L; m_1, m_2) Y_{L_1, m_1}(\mathbf{u}_i) \\ &\quad \times Y_{L_2, m_2}(\mathbf{u}_j) Y_{L, m_1 + m_2}^*(\hat{\mathbf{r}}_{ij}), \end{aligned} \quad (7)$$

where $C(L_1, L_2, L; m_1, m_2)$ denotes Clebsch–Gordan coefficients and the expansion coefficients, $c_{L_1, L_2, L}(r_{ij})$, only depend on the intermolecular distance r_{ij} . For a uniaxial phase of uniaxial molecules the ODF can be expanded in Legendre polynomials,

$$f_0(\mathbf{u}_j) = \sum_L \frac{2L+1}{4\pi} \langle P_L \rangle P_L(\cos \beta_j), \quad (8)$$

where the expansion coefficients are the order parameters, $\langle P_L \rangle$, which measure the degree of orientational order in the sample. We note that for molecules with ‘shape polarity’ L_1 , L_2 and L in Eqs. (7) and (8) can assume not only even, but all integer values. When introducing the expansions (7) and (8) into Eqs. (5) and (6) we are able to perform analytically all the solid angle integrals over the spherical harmonics [12]. Furthermore, from the symmetry properties of the Kronecker symbols and the Clebsch–Gordan coefficients [12] the multi-summations can be reduced to single series expansions. The *splay* flexoelectric coefficient then reads

$$\begin{aligned} e_{11} = & \sqrt{\frac{2\pi}{3}} \rho^2 p \sum_L \sqrt{(2L+1) \frac{(L+1)!}{(L-1)!}} \\ & \times \left\{ \sqrt{(2L-1)} C(L-1, L, 1; 0, 1) I_{L-1, L, 1}^3 \right. \\ & \times \left[[C(L-1, 1, L-2; 0, 0)]^2 \langle P_{L-2} \rangle \langle P_L \rangle \right. \\ & + [C(L-1, 1, L-1; 0, 0)]^2 \langle P_{L-1} \rangle \langle P_L \rangle \\ & + [C(L-1, 1, L; 0, 0)]^2 \langle P_L \rangle^2 \left. \right] \\ & + \sqrt{(2L+3)} C(L+1, L, 1; 0, 1) I_{L+1, L, 1}^3 \\ & \times \left[[C(L+1, 1, L; 0, 0)]^2 \langle P_L \rangle^2 \right. \\ & + [C(L+1, 1, L+1; 0, 0)]^2 \langle P_L \rangle \langle P_{L+1} \rangle \\ & + [C(L+1, 1, L+2; 0, 0)]^2 \langle P_L \rangle \langle P_{L+2} \rangle \left. \right] \left. \right\} \\ = & \sqrt{2\pi} \rho^2 p \left[(\sqrt{2} I_{0,1,1}^3 + \frac{2}{5} I_{2,1,1}^3) \langle P_1 \rangle^2 \right. \\ & \left. - I_{1,2,1}^3 (\langle P_2 \rangle + 2 \langle P_2 \rangle^2) + \dots \right], \quad (9) \end{aligned}$$

whereas the *bend* flexoelectric coefficient becomes

$$\begin{aligned} e_{33} = & \sqrt{\frac{2\pi}{3}} \rho^2 p \sum_L \sqrt{(2L+1) \frac{(L+1)!}{(L-1)!}} \\ & \times \left\{ \sqrt{(2L-1)} C(L-1, L, 1; 1, -1) I_{L-1, L, 1}^3 \right. \\ & \times \left[C(L-1, 1, L-2; 0, 0) \right. \\ & \times C(L-1, 1, L-2; 1, -1) \langle P_{L-2} \rangle \langle P_L \rangle \\ & + C(L-1, 1, L; 0, 0) \\ & \times C(L-1, 1, L; 1, -1) \langle P_L \rangle^2 \left. \right] \\ & + \sqrt{(2L+1)} C(L, L, 1; 1, -1) C(L, 1, L; 0, 0) \\ & \times C(L, 1, L; 1, -1) I_{L, L, 1}^3 \langle P_L \rangle^2 \\ & + \sqrt{(2L+3)} C(L+1, L, 1; 1, -1) I_{L+1, L, 1}^3 \\ & \times \left[C(L+1, 1, L; 0, 0) \right. \\ & \times C(L+1, 1, L; 1, -1) \langle P_L \rangle^2 \\ & + C(L+1, 1, L+2; 0, 0) \\ & \times C(L+1, 1, L+2; 1, -1) \langle P_L \rangle \langle P_{L+2} \rangle \left. \right] \left. \right\} \\ = & \sqrt{2\pi} \rho^2 p \left[-\frac{3}{5} I_{2,1,1}^3 \langle P_1 \rangle^2 + I_{1,2,1}^3 \right. \\ & \left. \times (-\langle P_2 \rangle + \langle P_2 \rangle^2) + \dots \right], \quad (10) \end{aligned}$$

where

$$I_{L_1, L_2, L}^3 = \int dr_{ij} r_{ij}^3 c_{L_1, L_2, L}(r_{ij}) \quad (11)$$

denote radial integrals of the *third* moments of the DPCF expansion coefficients. Similar series expansions as (9) and (10), based upon the Poniewierski–Stecki expressions [9] allow the evaluation of the Frank elastic constants [13,14]. Unlike the flexoelectric coefficients derived above, the elastic constants turn out to depend on the *fourth* moments of the DPCF.

3. Monte Carlo simulations for pear-shaped molecules

In order to evaluate the general expressions (9) and (10) we need to insert data for the scalar order parameters and the DPCF. We obtain these quantities by performing Monte Carlo simulations for a particular model of pear-shaped molecules. The ‘shape polarity’ is achieved by combining an ellipsoidal Gay–Berne (GB) [17] and a spherical Lennard-Jones

(LJ) center which are rigidly connected. Thus in our model each molecule consists of two sites, and therefore the total interaction $U(1,2)$ between the pair of molecules 1 and 2 is the sum of four contributions,

$$U(1,2) = U(\text{GB1,GB2}) + U(\text{LJ1,LJ2}) \\ + U(\text{GB1,LJ2}) + U(\text{LJ1,GB2}). \quad (12)$$

The two GB sites interact with the potential $U(\text{GB1,GB2})$ according to [18], which is identical in form to the original Gay–Berne potential function with length-to-width ratio 3:1 (see Ref. [17] for details), but with the parametrization $\kappa = 3$, $\kappa' = 5$, $\mu = 1$, $\nu = 3$, which exhibits a wider nematic range compared to the original version [17,18]. (All physical quantities will be expressed in reduced units, marked by an asterisk *, which are referred to the energy and length units, ϵ_0 and σ_0 , of the GB potential [17].) The standard 12-6 LJ potential is used to model the interaction $U(\text{LJ1,LJ2})$ between the spherical sites. Whereas its well depth is kept constant at unity ($\epsilon_{\text{LJ}}^* = 1$), the diameter σ_{LJ}^* of the LJ site is a parameter in our model that is varied in order to change the molecular steric dipole. We choose the two values $\sigma_{\text{LJ}}^* = 1.0$ and 1.1 and place the Lennard-Jones sphere along the long axis of the GB ellipsoid, so that their ends coincide, giving an intramolecular site distance of $d^* = 1.0$ or 0.95 , respectively. Reasonably, the steric dipole moment $p^* = p/(\epsilon_0 \sigma_0^4)$ should increase with both the volume of the LJ site and the GB–LJ intramolecular site distance as $p^* = (4\pi/3) \epsilon_{\text{LJ}}^* \sigma_{\text{LJ}}^{*3} d^*$. For our choice of parameters this definition yields, respectively, $p^* = 0.524$ and 0.662 . The last two terms in (12) account for the interaction between a GB and a LJ site. Their form has been derived [19] by generalizing to dissimilar particles the biaxial GB potential developed in [20].

We have investigated the model of shape asymmetry introduced above by employing Monte Carlo simulations at constant pressure $P^* = P\sigma_0^3/\epsilon_0$ and temperature $T^* = kT/\epsilon_0$ for a system of $N = 1000$ pear-shaped molecules. Interestingly, when starting from the nematic phase of the GB potential [18] at $P^* = 7$ and $T^* = 2.2, \dots, 3.5$, the effect of the additional LJ center is to suppress the existence of this phase, instead we find a direct transition from a highly ordered smectic *A* phase to the isotropic

phase. When increasing the pressure a relatively narrow nematic region can be found. Therefore we performed the *NPT* Monte Carlo simulations at $P^* = 10$ and various temperatures in the nematic phase of our model. For each state point the simulation runs consisted of at least 40 000 equilibration cycles, followed by 120 000–400 000 production cycles.

To analyze the simulation data we have extracted structural properties which, in turn, were used as input quantities to evaluate elastic and flexoelectric coefficients. In particular, the order parameters, $\langle P_L \rangle = \langle P_L(\mathbf{n} \cdot \mathbf{u}_i) \rangle_i$, were evaluated according to the procedure developed in [21]. The full pair distribution function (PDF) accounts for spatial correlations of pairs of molecules in the sample, taking into account the orientations of both their axes and their center of mass separation vectors. Its orientational dependence is analyzed most conveniently in terms of an expansion into rotational invariant functions, equivalent to the spherical harmonic expansion Eq. (7). Here we use the definition of basis functions $S_{L_1, L_2, L}(\mathbf{u}_i, \mathbf{u}_j, \hat{\mathbf{r}}_{ij})$ introduced by Stone [22]. The full PDF is determined by the infinite set of Stone expansion coefficients that can be calculated as

$$S_{L_1, L_2, L}(r_{ij}) = \frac{1}{\rho} \langle \delta(r_{ij} - r_{12}) \\ \times S_{L_1, L_2, L}(\mathbf{u}_1, \mathbf{u}_2, \hat{\mathbf{r}}_{12}) \rangle_{12}. \quad (13)$$

We calculate all Stone functions (13) up to *fourth* rank ($L_1, L_2 \leq 4$), even if the structure of the fluid is revealed already by the first and second rank functions. Indeed, the lowest order at which all terms enter the series expansions (9) and (10) is $L = 4$. Analogous calculations of elastic constants show that the fourth order theory is necessary to remove the *splay-bend degeneracy* [13,14], thus providing more realistic results. Whereas the order parameters $\langle P_L \rangle$ are directly accessible from the simulations, the DPCF, $c(\mathbf{r}_{ij}, \mathbf{u}_i, \mathbf{u}_j)$, is related to the total pair correlation function (TPCF), $h(\mathbf{r}_{ij}, \mathbf{u}_i, \mathbf{u}_j)$, via the Ornstein-Zernike (OZ) integral equation,

$$c(\mathbf{r}_{ij}, \mathbf{u}_i, \mathbf{u}_j) = h(\mathbf{r}_{ij}, \mathbf{u}_i, \mathbf{u}_j) + \rho \sum_L \frac{2L+1}{4\pi} \langle P_L \rangle \\ \times \int d\mathbf{r}_k d\mathbf{u}_k c(\mathbf{r}_{ik}, \mathbf{u}_i, \mathbf{u}_k) \\ \times P_L(\mathbf{n} \cdot \mathbf{u}_k) h(\mathbf{r}_{kj}, \mathbf{u}_k, \mathbf{u}_j). \quad (14)$$

Table 1

Thermodynamic quantities and scalar order parameters according to the Monte Carlo simulations. T^* and ρ^* are temperature and pressure, respectively. $\langle P_2 \rangle$ and $\langle P_4 \rangle$ denote the even rank orientational order parameters. The data include the nematic range of the two model systems with molecular steric dipole $p^* = 0.524$ (upper part) and $p^* = 0.662$ (lower part)

T^*	ρ^*	$\langle P_2 \rangle$	$\langle P_4 \rangle$
2.95	0.286 ± 0.001	0.788 ± 0.013	0.506 ± 0.021
3.00	0.284 ± 0.001	0.768 ± 0.015	0.457 ± 0.026
3.05	0.283 ± 0.001	0.733 ± 0.019	0.428 ± 0.032
3.10	0.281 ± 0.001	0.712 ± 0.017	0.367 ± 0.021
3.15	0.279 ± 0.001	0.682 ± 0.023	0.346 ± 0.026
3.20	0.278 ± 0.001	0.670 ± 0.023	0.317 ± 0.023
3.30	0.274 ± 0.001	0.543 ± 0.047	0.187 ± 0.035
3.40	0.267 ± 0.001	0.058 ± 0.040	0.005 ± 0.015
3.10	0.274 ± 0.001	0.691 ± 0.018	0.393 ± 0.024
3.15	0.272 ± 0.001	0.663 ± 0.020	0.334 ± 0.018
3.20	0.269 ± 0.001	0.523 ± 0.067	0.304 ± 0.018
3.30	0.264 ± 0.001	0.186 ± 0.028	0.035 ± 0.028
3.40	0.262 ± 0.001	0.074 ± 0.043	0.001 ± 0.014

In Eq. (14) the ODF $f(\mathbf{u}_k)$ is expressed by its Legendre polynomial expansion (8). The TPCF, h , which is derived from the pair distribution function (PDF), g , as $h = g - 1$, can be directly obtained from simulations. Taking the Monte Carlo data for the TPCF as an input, it is possible to obtain an iterative solution for the DPCF. We start keeping only $L = 0$ in the summation in (14) approximating $f(\mathbf{u}_k)$ by its isotropic part $1/(4\pi)$, while retaining the full dependence on the molecular orientations in the TPCF and DPCF. With this restriction the OZ equation can be solved as shown by Blum [15]. We applied this procedure according to the outlines given elsewhere [16]. The resulting DPCF expansion coefficients, $c_{L_1, L_2, L}(r_{ij})$, decay to zero to $\mathcal{O}(10^{-6})$ within the range of the intermolecular potential. Small longer range fluctuations are neglected by restricting the upper integration limit in (11) to the potential cutoff radius ($r_{\text{cut}}^* = 5$). Ideally, the DPCF should be evaluated at each temperature. However, unlike the TPCF, the DPCF is expected to be only weakly dependent on temperature [23], thus we have preferred to choose only $T^* = 3.00$ (for $p^* = 0.524$) and $T^* = 3.10$ (for $p^* = 0.662$), respectively, where the statistics of our calculations is particularly satisfactory. In order to check the validity of the isotropic approximation to

the OZ equation, we evaluated the convolution kernel in (14), inserting the TPCF and order parameters from the simulations as well as the DPCF obtained from the isotropic OZ equation. The convolution integral was computed numerically first in the isotropic approximation, keeping only $L = 0$ in (14). Afterwards, higher rank corrections were taken into account. The corrections retaining terms $L = 0, 1, 2$ turned out to be less than 1%. Therefore we conclude that neglecting the anisotropy of $f(\mathbf{u}_k)$ in (14) should have only a minor influence on our results.

4. Results

We start the analysis of the simulation results by investigating the temperature dependence of the scalar order parameters, $\langle P_L \rangle$, for the two systems of pear-shaped molecules with steric dipole $p^* =$

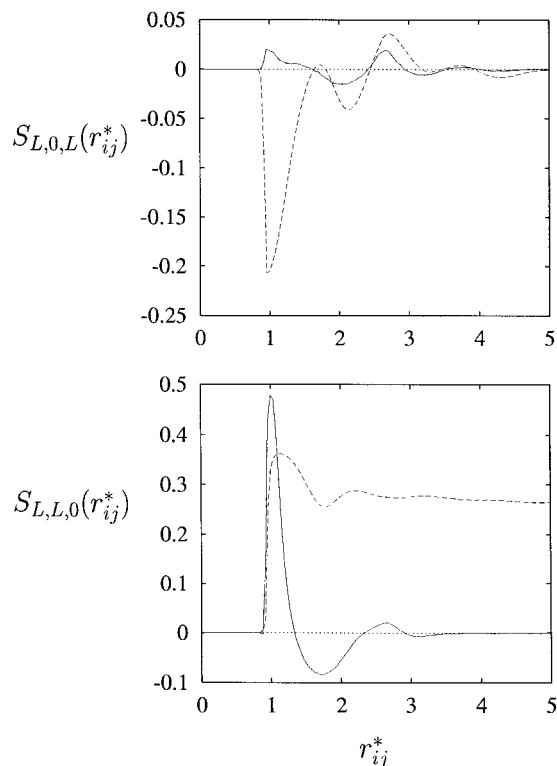


Fig. 1. Averaged Stone rotational invariants corresponding to temperature $T^* = 3.00$ and steric dipole $p^* = 0.524$. Upper part: $S_{101}(r_{ij}^*)$ (solid), $S_{202}(r_{ij}^*)$ (dashed); lower part: $S_{110}(r_{ij}^*)$ (solid), $S_{220}(r_{ij}^*)$ (dashed).

0.662 and $p^* = 0.524$. First of all, we mention that the odd rank order parameters ($L = 1, 3$) are almost zero, i.e., of order $1/\sqrt{N}$. This gives some hints already that there is *no mesoscopic polarization* in our system. We shall analyze this feature in more detail later on. In Table 1 we present the even rank order parameters $\langle P_2 \rangle$ and $\langle P_4 \rangle$. For both systems, the orientational order is decreasing with increasing temperature until the isotropic phase is formed at $T^* = 3.40$. However, the molecules with the stronger steric dipole are slightly less ordered in the nematic phase, hinting that the molecular shape asymmetry tends to reduce the degree of orientational order. Moreover, it restricts the range of the nematic phase. For temperatures below $T^* = 3.10$, the system with $p^* = 0.662$ clearly reveals a smectic layering. This tendency could be confirmed by further calculations with an even stronger shape asymmetry ($p^* = 0.814$), for which the nematic phase vanishes completely.

In order to examine more thoroughly the molecular organization in the nematic phase, in Fig. 1 we plot some selected rotational invariants [22], corresponding to $p^* = 0.524$ and $T^* = 3.00$. The averaged basis functions $S_{L,0,L}(r_{ij}^*)$ and $S_{L,L,0}(r_{ij}^*)$ provide detailed information on the relative orientation of molecular pairs. Here the nearest neighbour peaks are of particular interest. Importantly, due to the shape asymmetry of the pear molecules also the first rank invariants are non-zero. Especially, we note the positive values of the function $S_{1,1,0}(r_{ij}^*)$, indicating that neighbouring molecules prefer to align *antiparallel*. Such molecular organization, as stated above, leads to vanishing odd rank order parameters and prevents the formation of a polarization on a larger scale. Therefore, for our model system flexoelectric effects are expected to be quite small. The preference of antiparallel alignment can be partly observed even from a snapshot of the molecular configuration (Fig. 2).

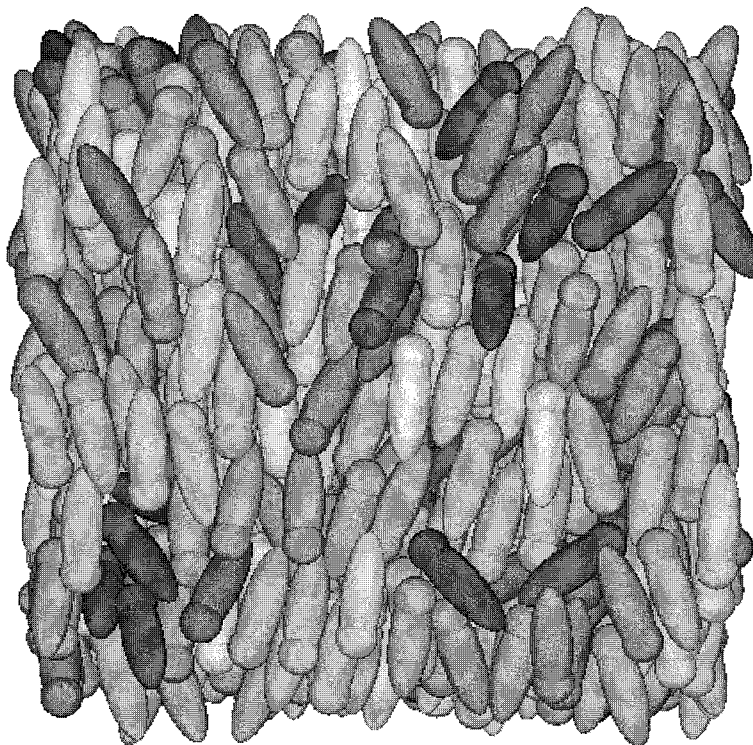


Fig. 2. Molecular configuration corresponding to temperature $T^* = 3.00$ and steric dipole $p^* = 0.524$. The gray level indicates the angle between the individual molecule and the director (*light* parallel ... *dark* perpendicular).

Table 2

Order parameter dependence of elastic constants K_{ii}^* and flexoelectric coefficients e_{ii}^* for the model system with molecular steric dipole $p^* = 0.524$

$\langle P_2 \rangle$	K_{11}^*	K_{22}^*	K_{33}^*	e_{11}^*	e_{33}^*
0.788 ± 0.013	18.30 ± 0.04	18.58 ± 0.04	17.11 ± 0.04	0.13 ± 0.01	0.001 ± 0.01
0.768 ± 0.015	15.75 ± 0.04	16.07 ± 0.04	14.69 ± 0.04	0.12 ± 0.02	0.001 ± 0.02
0.733 ± 0.019	14.31 ± 0.06	14.64 ± 0.06	13.34 ± 0.06	0.11 ± 0.03	0.001 ± 0.03
0.712 ± 0.017	11.46 ± 0.05	11.83 ± 0.05	10.67 ± 0.05	0.09 ± 0.02	0.001 ± 0.02
0.682 ± 0.023	10.51 ± 0.06	10.86 ± 0.06	9.77 ± 0.06	0.08 ± 0.03	0.001 ± 0.03
0.670 ± 0.023	9.29 ± 0.04	9.65 ± 0.04	8.64 ± 0.04	0.07 ± 0.03	0.001 ± 0.03
0.543 ± 0.047	4.42 ± 0.05	4.70 ± 0.05	4.12 ± 0.05	0.04 ± 0.03	0.001 ± 0.03
0.058 ± 0.040	0.03 ± 0.06	0.03 ± 0.06	0.03 ± 0.06	0.001 ± 0.03	0.001 ± 0.03

We now turn to the dependence of the elastic and flexoelectric coefficients on the order parameter $\langle P^2 \rangle$. The tables contain the Frank elastic constants $K_{ii}^* = K_{ii} \sigma_0 / \epsilon_0$ and the flexoelectric coefficients $e_{ii}^* = e_{ii} \sigma_0^2 / \epsilon_0$ for the two model systems with steric dipole $p^* = 0.524$ (Table 2) and $p^* = 0.662$ (Table 3).

The slightly different degree of order discussed above does not have a large influence on the *absolute* values of the elastic constants. Significantly, the pear-shaped molecules reveal an unusual elastic anisotropy. Whereas for the elastic constants of rod-like molecules we commonly find $K_{33}^* > K_{11}^* > K_{22}^* > 0$ [13,24], the additional LJ center has considerable influence on the *relative* importance of elastic distortions. Unlike the case of symmetric molecules, we find that the shape polarity favours *bend* deformations: the tables reveal K_{33}^* to be the smallest of the elastic constants. For both model systems we find an anisotropy as $K_{22}^* > K_{11}^* > K_{33}^* > 0$, which is opposite to what is known for rod-like molecules and rather close to discotic systems [14]. A possible explanation could be again the locally preferred anti-

parallel alignment of the molecules. *Splay* and *twist* distortions force two neighbouring molecules to disrupt this arrangement, whereas *bend* deformations act along the direction of the molecular axes and thus are more favorable.

Next we discuss the flexoelectric coefficients for the two model systems. As already stated above, flexoelectric effects are supposed to be rather small, which is reflected by the numerical values of the corresponding coefficients. In particular, e_{33}^* is even one order of magnitude smaller than e_{11}^* . The smallness of e_{33}^* , which falls within the error bar of our calculations, nevertheless suggests that there is hardly any *bend* flexoelectric effect. Indeed, Meyer had pointed out already that for pear-shaped molecules the polarization couples to a *splay* distortion, whereas a banana shape of the molecules should be necessary in order to produce a *bend* flexoelectric effect [1]. Our calculations are in qualitative agreement with these arguments and, in addition, we can provide a quantitative estimate on the relative importance of flexoelectric deformations. Experimental data for e_{11}^* and e_{33}^* are scarce and they are spread over a wide

Table 3

Order parameter dependence of elastic constants K_{ii}^* and flexoelectric coefficients e_{ii}^* for the model system with molecular steric dipole $p^* = 0.662$

$\langle P_2 \rangle$	K_{11}^*	K_{22}^*	K_{33}^*	e_{11}^*	e_{33}^*
0.691 ± 0.018	11.09 ± 0.02	11.98 ± 0.02	10.01 ± 0.02	0.14 ± 0.02	-0.001 ± 0.02
0.663 ± 0.020	7.64 ± 0.02	8.38 ± 0.02	6.90 ± 0.02	0.11 ± 0.02	-0.001 ± 0.02
0.523 ± 0.067	5.35 ± 0.04	5.93 ± 0.04	4.84 ± 0.04	0.08 ± 0.03	-0.001 ± 0.03
0.186 ± 0.028	0.38 ± 0.02	0.45 ± 0.02	0.35 ± 0.02	0.01 ± 0.02	-0.001 ± 0.02
0.074 ± 0.043	0.01 ± 0.01	0.02 ± 0.01	0.01 ± 0.01	0.001 ± 0.01	-0.001 ± 0.01

range, depending on the method used to detect flexoelectric effects. Considering the fact that most data are available for MBBA [25–34] which is far from being a pear-shaped molecule it is very difficult to relate the calculations for our idealized model systems to real experiments in a quantitative way. However, concerning the rôle of shape asymmetry, a general trend can be extracted from our investigations. When we compare the two systems it is apparent that an increase of the steric dipole leads to a considerable increase of the *splay* flexoelectric coefficient, whereas the average elastic constant is barely affected by this change in molecular shape. Most experiments yield the ratio between combinations of the flexoelectric coefficients and an elastic constant $(e_{11} \pm e_{33})/K$. By performing experiments for a series of molecules that are only slightly different in their asymmetry the interplay between shape polarity and the magnitude of flexoelectric effects should be directly accessible.

In summary we have shown that flexoelectric coefficients can be obtained by computer simulations, starting from a simple molecular model which allows controlled asymmetric deformations.

Acknowledgements

We wish to acknowledge support from CNR, MURST, University of Bologna and the EU (TMR-FMRX CT970121) and, in particular, a M. Curie TMR grant to J. Stelzer.

References

- [1] R.B. Meyer, Phys. Rev. Lett. 22 (1969) 918.
- [2] J. Prost, J.P. Marcerou, J. de Physique 38 (1977) 315.
- [3] J.P. Marcerou, J. Prost, Mol. Cryst. Liq. Cryst. 58 (1980) 259.
- [4] M.A. Osipov, Sov. Phys. JETP 56 (1983) 1167.
- [5] M.A. Osipov, J. de Physique Lett. 45 (1984) 823.
- [6] J.P. Straley, Phys. Rev. A 14 (1976) 1835.
- [7] V.B. Nemtsov, M.A. Osipov, Sov. Phys. Crystallogr. 31 (1986) 125.
- [8] M.D. Lipkin, S.A. Rice, U. Mohanty, J. Chem. Phys. 82 (1985) 472.
- [9] A. Poniewierski, J. Stecki, Mol. Phys. 38 (1979) 1931.
- [10] B. Tjijto-Margo, G.T. Evans, M.P. Allen, D. Frenkel, J. Phys. Chem. 96 (1992) 3942.
- [11] F.C. Frank, Disc. Faraday Soc. 25 (1958) 19.
- [12] C.G. Gray, K.E. Gubbins, Theory of Molecular Fluids, vol. 1, Oxford University Press, Oxford, 1984.
- [13] J. Stelzer, L. Longa, H.-R. Trebin, J. Chem. Phys. 103 (1995) 3098; 107 (1997) 1295E.
- [14] J. Stelzer, M.A. Bates, L. Longa, G.R. Luckhurst, J. Chem. Phys. 107 (1997) 7483.
- [15] L. Blum, J. Chem. Phys. 58 (1973) 3295.
- [16] M.P. Allen, C. Mason, E. de Miguel, J. Stelzer, Phys. Rev. E 52 (1995) R25.
- [17] J.G. Gay, B.J. Berne, J. Chem. Phys. 74 (1981) 3316.
- [18] R. Berardi, A.P.J. Emerson, C. Zannoni, J. Chem. Soc., Faraday Trans. 89 (1993) 4069.
- [19] R. Berardi, C. Fava, C. Zannoni, Chem. Phys. Lett. 297 (1998) 8.
- [20] R. Berardi, C. Fava, C. Zannoni, Chem. Phys. Lett. 236 (1995) 462.
- [21] F. Biscarini, C. Chiccoli, P. Pasini, F. Semeria, C. Zannoni, Phys. Rev. Lett. 75 (1995) 1803.
- [22] A.J. Stone, Mol. Phys. 36 (1978) 241.
- [23] M.P. Allen, M.A. Warren, Phys. Rev. Lett. 78 (1997) 1291.
- [24] M.P. Allen, M.A. Warren, M.R. Wilson, A. Sauron, W. Smith, J. Chem. Phys. 105 (1996) 2850.
- [25] D. Schmidt, M. Schadt, W. Helfrich, Z. Naturforsch. A 27 (1972) 277.
- [26] J. Prost, P.S. Pershan, J. Appl. Phys. 47 (1976) 2298.
- [27] A.S. Vasilevskaya, A.V. Kaznachev, A.S. Sonin, Sov. Phys. Solid State 24 (1982) 2118.
- [28] I. Dozov, P. Martinot-Lagarde, G. Durand, J. de Physique Lett. 43 (1982) 365.
- [29] I. Dozov, I. Penchev, P. Martinot-Lagarde, G. Durand, Ferroelectrics Lett. 2 (1984) 135.
- [30] N.V. Madhusudhana, G. Durand, J. de Physique Lett. 46 (1985) 195.
- [31] G. Barbero, P. Taverna-Valabrega, R. Bartolino, B. Valenti, Liq. Cryst. 1 (1986) 483.
- [32] B. Valenti, C. Bertoni, G. Barbero, P. Taverna-Valabrega, R. Bartolino, Mol. Cryst. Liq. Cryst. 146 (1987) 307.
- [33] L.M. Blinov, L.A. Beresnev, S.A. Davidyan, S.G. Kononov, S.V. Yablonsky, Ferroelectrics 84 (1988) 365.
- [34] G. Barbero, A.N. Chuvyrov, A.P. Krekhov, O.A. Scaldin, J. Appl. Phys. 69 (1991) 6343.